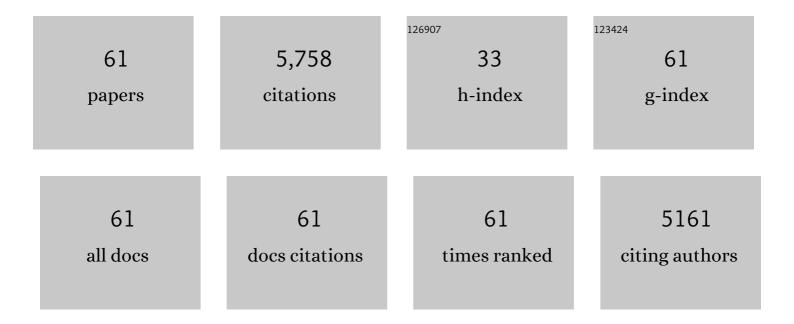
## Michael S Middleton

List of Publications by Year in descending order

Source: https://exaly.com/author-pdf/4429324/publications.pdf Version: 2024-02-01



#	Article	IF	CITATIONS
1	<i>In vivo</i> characterization of the liver fat <sup>1</sup> H MR spectrum. NMR in Biomedicine, 2011, 24, 784-790.	2.8	452
2	Utility of magnetic resonance imaging versus histology for quantifying changes in liver fat in nonalcoholic fatty liver disease trials. Hepatology, 2013, 58, 1930-1940.	7.3	434
3	Nonalcoholic Fatty Liver Disease: MR Imaging of Liver Proton Density Fat Fraction to Assess Hepatic Steatosis. Radiology, 2013, 267, 422-431.	7.3	410
4	Relaxation effects in the quantification of fat using gradient echo imaging. Magnetic Resonance Imaging, 2008, 26, 347-359.	1.8	356
5	Nonalcoholic Fatty Liver Disease: Diagnostic and Fat-Grading Accuracy of Low-Flip-Angle Multiecho Gradient-Recalled-Echo MR Imaging at 1.5 T. Radiology, 2009, 251, 67-76.	7.3	287
6	Estimation of Hepatic Proton-Density Fat Fraction by Using MR Imaging at 3.0 T. Radiology, 2011, 258, 749-759.	7.3	259
7	Accuracy of MR Imaging–estimated Proton Density Fat Fraction for Classification of Dichotomized Histologic Steatosis Grades in Nonalcoholic Fatty Liver Disease. Radiology, 2015, 274, 416-425.	7.3	239
8	GS-0976 Reduces Hepatic Steatosis and Fibrosis Markers in Patients With Nonalcoholic Fatty Liver Disease. Gastroenterology, 2018, 155, 1463-1473.e6.	1.3	238
9	Linearity, Bias, and Precision of Hepatic Proton Density Fat Fraction Measurements by Using MR Imaging: A Meta-Analysis. Radiology, 2018, 286, 486-498.	7.3	225
10	Agreement Between Magnetic Resonance Imaging Proton Density Fat Fraction Measurements and Pathologist-Assigned Steatosis Grades of Liver Biopsies From Adults With Nonalcoholic Steatohepatitis. Gastroenterology, 2017, 153, 753-761.	1.3	209
11	Effect of PRESS and STEAM sequences on magnetic resonance spectroscopic liver fat quantification. Journal of Magnetic Resonance Imaging, 2009, 30, 145-152.	3.4	201
12	Effect of a Low Free Sugar Diet vs Usual Diet on Nonalcoholic Fatty Liver Disease in Adolescent Boys. JAMA - Journal of the American Medical Association, 2019, 321, 256.	7.4	163
13	Acetyl-CoA Carboxylase Inhibitor GS-0976 for 12 Weeks Reduces Hepatic De Novo Lipogenesis and Steatosis in Patients With Nonalcoholic Steatohepatitis. Clinical Gastroenterology and Hepatology, 2018, 16, 1983-1991.e3.	4.4	153
14	Longitudinal correlations between MRE, MRI-PDFF, and liver histology in patients with non-alcoholic steatohepatitis: Analysis of data from a phase II trial of selonsertib. Journal of Hepatology, 2019, 70, 133-141.	3.7	149
15	Magnetic resonance imaging and liver histology as biomarkers of hepatic steatosis in children with nonalcoholic fatty liver disease. Hepatology, 2015, 61, 1887-1895.	7.3	138
16	Reproducibility of MRIâ€determined proton density fat fraction across two different MR scanner platforms. Journal of Magnetic Resonance Imaging, 2011, 34, 928-934.	3.4	130
17	Prevalence of Nonalcoholic Fatty Liver Disease in Children with Obesity. Journal of Pediatrics, 2019, 207, 64-70.	1.8	130
18	Magnetic Resonance Imaging Proton Density Fat Fraction Associates With Progression of Fibrosis in Patients With Nonalcoholic Fatty Liver Disease. Gastroenterology, 2018, 155, 307-310.e2.	1.3	113

#	Article	IF	CITATIONS
19	Diagnostic accuracy of magnetic resonance imaging hepatic proton density fat fraction in pediatric nonalcoholic fatty liver disease. Hepatology, 2018, 67, 858-872.	7.3	112
20	Magnetic resonance elastography measured shear stiffness as a biomarker of fibrosis in pediatric nonalcoholic fatty liver disease. Hepatology, 2017, 66, 1474-1485.	7.3	103
21	In Children With Nonalcoholic Fatty Liver Disease, Cysteamine Bitartrate Delayed Release Improves Liver Enzymes but Does Not Reduce Disease Activity Scores. Gastroenterology, 2016, 151, 1141-1154.e9.	1.3	100
22	Spatial distribution of MRI-determined hepatic proton density fat fraction in adults with nonalcoholic fatty liver disease. Journal of Magnetic Resonance Imaging, 2014, 39, 1525-1532.	3.4	85
23	Imaging Outcomes of Liver Imaging Reporting and Data System Version 2014 Category 2, 3, and 4 Observations Detected at CT and MR Imaging. Radiology, 2016, 281, 129-139.	7.3	85
24	Automated CT and MRI Liver Segmentation and Biometry Using a Generalized Convolutional Neural Network. Radiology: Artificial Intelligence, 2019, 1, 180022.	5.8	78
25	Diagnosis of fatty liver with MR imaging. Journal of Magnetic Resonance Imaging, 1992, 2, 463-471.	3.4	60
26	Intra- and inter-examination repeatability of magnetic resonance spectroscopy, magnitude-based MRI, and complex-based MRI for estimation of hepatic proton density fat fraction in overweight and obese children and adults. Abdominal Imaging, 2015, 40, 3070-3077.	2.0	57
27	Associations between histologic features of nonalcoholic fatty liver disease (NAFLD) and quantitative diffusionâ€weighted MRI measurements in adults. Journal of Magnetic Resonance Imaging, 2015, 41, 1629-1638.	3.4	57
28	Accuracy and the effect of possible subjectâ€based confounders of magnitudeâ€based MRI for estimating hepatic proton density fat fraction in adults, using MR spectroscopy as reference. Journal of Magnetic Resonance Imaging, 2016, 43, 398-406.	3.4	52
29	Inter-examination precision of magnitude-based MRI for estimation of segmental hepatic proton density fat fraction in obese subjects. Journal of Magnetic Resonance Imaging, 2014, 39, 1265-1271.	3.4	47
30	Intravenous Gadoxetate Disodium Administration Reduces Breath-holding Capacity in the Hepatic Arterial Phase: A Multi-Center Randomized Placebo-controlled Trial. Radiology, 2017, 282, 361-368.	7.3	46
31	In vivo triglyceride composition of abdominal adipose tissue measured by <sup>1</sup> H MRS at 3T. Journal of Magnetic Resonance Imaging, 2017, 45, 1455-1463.	3.4	44
32	Effect of flip angle on the accuracy and repeatability of hepatic proton density fat fraction estimation by complex dataâ€based, T1â€independent, T2*â€corrected, spectrumâ€modeled MRI. Journal of Magnetic Resonance Imaging, 2014, 39, 440-447.	3.4	43
33	Linearity and Bias of Proton Density Fat Fraction as a Quantitative Imaging Biomarker: A Multicenter, Multiplatform, Multivendor Phantom Study. Radiology, 2021, 298, 640-651.	7.3	39
34	Quantifying Abdominal Adipose Tissue and Thigh Muscle Volume and Hepatic Proton Density Fat Fraction: Repeatability and Accuracy of an MR Imaging–based, Semiautomated Analysis Method. Radiology, 2017, 283, 438-449.	7.3	38
35	Repeatability and reproducibility of 2D and 3D hepatic MR elastography with rigid and flexible drivers at end-expiration and end-inspiration in healthy volunteers. Abdominal Radiology, 2017, 42, 2843-2854.	2.1	34
36	In vivo breathâ€hold <sup>1</sup> H MRS simultaneous estimation of liver proton density fat fraction, and <i>T</i> <sub>1</sub> and <i>T</i> <sub>2</sub> of water and fat, with a multiâ€TR, multiâ€TE sequence. Journal of Magnetic Resonance Imaging, 2015, 42, 1538-1543.	3.4	32

MICHAEL S MIDDLETON

#	Article	IF	CITATIONS
37	Evaluation of Liver Fibrosis Using Texture Analysis on Combined-Contrast-Enhanced Magnetic Resonance Images at 3.0T. BioMed Research International, 2015, 2015, 1-12.	1.9	28
38	Hepatic R2* is more strongly associated with proton density fat fraction than histologic liver iron scores in patients with nonalcoholic fatty liver disease. Journal of Magnetic Resonance Imaging, 2019, 49, 1456-1466.	3.4	28
39	MRI proton density fat fraction is robust across the biologically plausible range of triglyceride spectra in adults with nonalcoholic steatohepatitis. Journal of Magnetic Resonance Imaging, 2018, 47, 995-1002.	3.4	27
40	Accuracy of multiecho magnitudeâ€based MRI (Mâ€MRI) for estimation of hepatic proton density fat fraction (PDFF) in children. Journal of Magnetic Resonance Imaging, 2015, 42, 1223-1232.	3.4	25
41	Liver histology and diffusionâ€weighted MRI in children with nonalcoholic fatty liver disease: A MAGNET study. Journal of Magnetic Resonance Imaging, 2017, 46, 1149-1158.	3.4	25
42	Effects of intravenous gadolinium administration and flip angle on the assessment of liver fat signal fraction with opposedâ€phase and inâ€phase imaging. Journal of Magnetic Resonance Imaging, 2008, 28, 246-251.	3.4	22
43	MR Evaluation of Breast Implants. Radiologic Clinics of North America, 2014, 52, 591-608.	1.8	20
44	Feasibility of and agreement between MR imaging and spectroscopic estimation of hepatic proton density fat fraction in children with known or suspected nonalcoholic fatty liver disease. Abdominal Imaging, 2015, 40, 3084-3090.	2.0	20
45	Accuracy of PDFF estimation by magnitudeâ€based and complexâ€based MRI in children with MR spectroscopy as a reference. Journal of Magnetic Resonance Imaging, 2017, 46, 1641-1647.	3.4	19
46	Crossâ€sectional correlation between hepatic R2* and proton density fat fraction (PDFF) in children with hepatic steatosis. Journal of Magnetic Resonance Imaging, 2018, 47, 418-424.	3.4	19
47	Accuracy of common proton density fat fraction thresholds for magnitude- and complex-based chemical shift-encoded MRI for assessing hepatic steatosis in patients with obesity. Abdominal Radiology, 2020, 45, 661-671.	2.1	16
48	Dairy Fat Intake, Plasma Pentadecanoic Acid, and Plasma Isoâ€heptadecanoic Acid Are Inversely Associated With Liver Fat in Children. Journal of Pediatric Gastroenterology and Nutrition, 2021, 72, e90-e96.	1.8	16
49	Diagnostic Accuracy of Preoperative Gadoxetic Acid–enhanced 3-T MR Imaging for Malignant Liver Lesions by Using Ex Vivo MR Imaging–matched Pathologic Findings as the Reference Standard. Radiology, 2015, 276, 775-786.	7.3	14
50	MR elastography in nonalcoholic fatty liver disease: inter-center and inter-analysis-method measurement reproducibility and accuracy at 3T. European Radiology, 2022, 32, 2937-2948.	4.5	12
51	Temperatureâ€corrected proton density fat fraction estimation using chemical shiftâ€encoded MRI in phantoms. Magnetic Resonance in Medicine, 2021, 86, 69-81.	3.0	11
52	Assessment of a high‣NR chemicalâ€shiftâ€encoded MRI with complex reconstruction for proton density fat fraction (PDFF) estimation overall and in the lowâ€fat range. Journal of Magnetic Resonance Imaging, 2019, 49, 229-238.	3.4	9
53	The relationship between liver triglyceride composition and proton density fat fraction as assessed by 1 H MRS. NMR in Biomedicine, 2020, 33, e4286.	2.8	9
54	Effect of intravenous gadoxetate disodium and flip angle on hepatic proton density fat fraction estimation with six-echo, gradient-recalled-echo, magnitude-based MR imaging at 3T. Abdominal Radiology, 2017, 42, 1189-1198.	2.1	6

#	Article	IF	CITATIONS
55	Agreement between region-of-interest- and parametric map-based hepatic proton density fat fraction estimation in adults with chronic liver disease. Abdominal Radiology, 2017, 42, 833-841.	2.1	6
56	Magnetic resonance elastography biomarkers for detection of histologic alterations in nonalcoholic fatty liver disease in the absence of fibrosis. European Radiology, 2021, 31, 8408-8419.	4.5	6
57	Automated CNN–Based Analysis Versus Manual Analysis for MR Elastography in Nonalcoholic Fatty Liver Disease: Intermethod Agreement and Fibrosis Stage Discriminative Performance. American Journal of Roentgenology, 2022, 219, 224-232.	2.2	6
58	Evaluation of Quantitative Imaging Biomarkers for Earlyâ€phase Clinical Trials of Steatohepatitis in Adolescents. Journal of Pediatric Gastroenterology and Nutrition, 2020, 70, 99-105.	1.8	5
59	Repeatability and accuracy of various region-of-interest sampling strategies for hepatic MRI proton density fat fraction quantification. Abdominal Radiology, 2021, 46, 3105-3116.	2.1	5
60	Hepatic Steatosis is Negatively Associated with Bone Mineral Density in Children. Journal of Pediatrics, 2021, 233, 105-111.e3.	1.8	4
61	Prospective comparison of longitudinal change in hepatic proton density fat fraction (PDFF) estimated by magnitude-based MRI (MRI-M) and complex-based MRI (MRI-C). European Radiology, 2020, 30, 5120-5129.	4.5	2